Differential Brd4-bound enhancers drive critical sex differences in glioblastoma

N. Kfoury[1, #], Z. Qi[2, #], A. Yim[2], K. Berrett[3], S. Sankararaman[2], L. Broestl[1], X. Chen[2, 4], M. Wilkinson[2], J. Ippolito[5], J. Gertz[3], R. Mitra[2, †] and J. Rubin[1,6,†, *]

Affiliations:

[1] Department of Pediatrics, School of Medicine, Washington University in St. Louis.

[2] Department of Genetics, School of Medicine, Washington University in St. Louis.

[3] Department of Oncological Sciences, Huntsman Cancer Institute, University of Utah.

[4] Center for Genome Sciences and Systems Biology Washington University in St. Louis.

[5] Department of Radiology, School of Medicine, Washington University in St. Louis.

[6] Department of Neuroscience, School of Medicine, Washington University in St. Louis.

*Correspondence to: Joshua B. Rubin (Rubin_J@kids.wustl.edu) or Robi Mitra (rmitra@wustl.edu)

First co-authors

† Last co-authors

Abstract:

Sex differences in the incidence and severity of numerous human diseases, including cancer, are substantial and demand an understanding at a molecular level. In an established model of Glioblastoma (GBM), we discovered transcriptome-wide sexual dimorphism in patterns of gene-expression, H3K27ac marks (ChIP-seq) and large Brd4-bound enhancers (calling cards) of the type referred to as super/stretch enhancers. Genetic depletion or pharmacological inhibition of Brd4 reproducibly abrogated the sex differences in the GBM phenotype; male cells became less clonogenic, proliferative, and tumorigenic, while female cells became more clonogenic. Finally,

sexual dimorphism in Brd4 function was consistent with sex differences in the effect of low Brd4 expression on survival in GBM patients. These data establish for the first time that sex is an intrinsic element of cellular identity, and that it is driven by differential Brd4 activity, which renders male and female cells differentially sensitive to JQ1 treatment.

One Sentence Summary:

Sex-specific differences in GBM tumorigenic phenotype are achieved through differential Brd4 activity and can be reversed by treating cells with the Brd4 antagonist JQ1.

Main Text:

Until recently, most basic and clinical research has focused on investigating factors that influence disease susceptibility and progression without regard to sex. However, a mounting body of evidence has revealed significant sex-specific differences in incidence, age of onset, and outcome of numerous human diseases. These include cardiovascular diseases, asthma, autoimmune diseases, birth defects, neurological diseases, psychiatric disorders and cancers (*1*). This preponderance of sex differences in disease incidence and outcome led to the implementation of new guidelines by the NIH regarding inclusion of sex as a biological variable in all research.

Glioblastoma (GBM), the most common and aggressive form of brain cancer (*2, 3*), is more common in males regardless of race or region of the world (male to female incidence of 1.6:1) (*4-7*). The reasons for sex differences in GBM incidence are largely unknown. While sex differences in disease are often mediated through acute sex hormone actions, sex differences in malignant brain tumor rates are evident at all ages, suggesting that factors other than circulating sex hormones

underlie this discrepancy (*8*). Recently, our lab discovered that an established model of GBM involving combined loss of neurofibromin (NF1) and p53 function in murine neocortical astrocytes exhibits sex differences in *in vivo* tumorigenicity mimicking those observed in patients with GBM (*9*). Together, the human and mouse data suggest that male and female cells may be differentially sensitive to the transforming effects of specific oncogenic events.

Sexual differentiation is in large part an epigenetic phenomenon (*10*). Understanding how mechanisms of sexual differentiation blend with the genetics and epigenetics of tumorigenesis to shape cancer biology will be imperative to understanding the key processes that impart females with relative resistance and males with relative susceptibility to cancer. Here we show that sex differences in tumor phenotype arise through differential Brd4-bound enhancer usage in male and female GBM cells. The phenotypic differences between male and female GBM cells are abolished by knockdown of Brd4, or treatment with JQ1, a clinically available Brd4 inhibitor (*11*). Consistent with these data, we observe sex differences in the effects of low Brd4 expression on survival in male and female GBM patients. This is the first demonstration that differential Brd4 activity mediates cell intrinsic sex identity and sex differences in a cancer phenotype. Together with sex differences in JQ1 effects, these results strongly indicate that sex differences in disease biology translate into sex differences in therapeutic responses. This has broad implications for medicine.

Male and female GBM cells exhibit transcriptome-wide differences in gene expression

Based on our previous observation of sex-specific differences in the tumorigenic phenotype between male and female GBM cells (*9*), we first sought to characterize the male and female transcriptome. We profiled male and female GBM cells with RNA sequencing. For each condition, three biological replicates were performed; the data were highly reproducible (Pearson $r \geq 0.96$ for

all pairwise comparisons) (**Supplementary Figure 1A**) and indicated differential expression of 3846 transcripts (FDR < 0.05) (**Figure 1A** and **Supplementary Figure 1B**). Pathway enrichment analysis for the top 400 differentially regulated genes was performed using a combination of KEGG pathway and Genomatix Pathway System (GePS). Classification of these genes according to function revealed a significant number of relevant and important pathways including cell differentiation, cell proliferation, glioblastoma, tumor angiogenesis, metabolism, and DNA binding-transcription factors **(Figure 1B)**. Thus, there are global differences in male and female GBM cell transcriptomes in cancer relevant pathways, which we hypothesize, are due to differences in sex-specific enhancer activity.

A

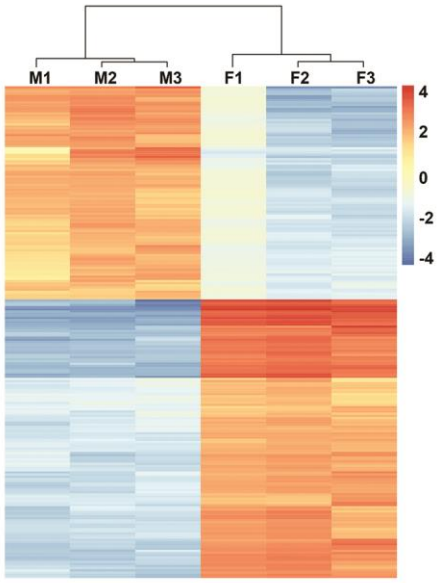

B

Pathway enrichment analysis for differentially regulated genes in male and female GBM cells*

Pathway description	*p*-value	# of Genes
Metabolic process	1.50E-02	176
Glioblastoma	0.00E+00	86
Cell proliferation	0.00E+00	69
Cell differentiation	0.00E+00	63
Cell death	0.00E+00	57
DNA binding-Transcription factors	0.00E+00	35
Tumor angiogenesis	0.00E+00	29

*Subset of pathway enrichment analysis

Figure 1: RNA profiling of male and female GBM cells reveals sexual dimorphism in cancer relevant pathways. RNA isolated from male and female GBM cells (n=3 each) was sequenced and results were analyzed. **(A)** Heat map depiction of differences in RNA abundance in male and female astrocytes (top 200 upregulated male/female genes and 200 downregulated male/female genes). **(B)** Subset of pathways significantly affected by sex. Adjusted *p*-values are shown.

Male and female GBM cells utilize different sets of Brd4-bound enhancers

To define the sex-specific enhancers that drive these transcriptional differences, we performed Chromatin Immunoprecipitation Sequencing (ChIP-seq) in male and female GBM cells to identify genomic regions enriched for H3K27 acetylation, a well-known marker of active enhancers. Three biological replicates were carried out and the correlation between replicates was $r^2 > 0.9$ for all pairwise comparisons **(Supplementary Figure 2A, 2B)**. Using established methods (*12*), we identified a total of 48881 and 51232 H3K27ac-enriched peaks in male and female GBM cells respectively. Of these, 10861 (22%) were male-specific and 13212 (26%) were female-specific **(Figure 2A)**. We then performed differential analysis between male and female cells and identified an additional 15976 differentially H3K27ac-enriched regions, as depicted in the heat map clustered by male and female **(Figure 2B)**. We correlated gene expression levels with H3K27ac binding and found that male upregulated genes are associated with H3K27ac enrichment in males compared to females, and vice versa for female upregulated genes (**Supplementary Figure 2C;** $p < 0.01$).

In order to prioritize enhancers for further analysis, we focused on highly active Brd4-bound enhancers, which have been named super- or stretch-enhancers. These enhancers have been shown to play key roles in establishing cell-identity and thus may be important in establishing sex differences. Furthermore, these enhancers bind up to 90% of Brd4 protein in the cell (*13-18*). Brd4 is an epigenetic reader that binds acetylated histones H3 and H4 throughout the entire cell cycle and is known to be deregulated in numerous cancers (*19*). Brd4 is thought to play a central role in cancer by promoting epithelial-to-mesenchymal transition, stem cell-like conversion, and pluripotency (*20-22*), and the pharmacological inhibition of this protein has shown therapeutic activity in a number of different cancer models (*11*, *23-26*). To investigate whether these highly

active Brd4-bound enhancers might play a role in establishing cell-intrinsic sex differences, we used transposon Calling Cards (*27, 28*) to identify enhancers differentially bound by Brd4. To do so, we fused the PB transposase to the C terminus of the Brd4 protein, endowing it with the ability to direct the insertion of the PB transposon into the genome close to Brd4 binding sites. Using this protocol, we mapped ~48,000 and ~30,000 unique insertions directed by the Brd4-PBase fusion for male and female samples respectively and identified 918 enhancers that bound significantly more Brd4 protein in males and 1171 enhancers that bound significantly more Brd4 protein in females.

To determine whether the enhancers that bound Brd4 in a sex specific manner also displayed differential H3K27ac, we first stitched H3K27ac-enriched individual enhancers within a distance of 12.5kb of each other to generate broad enhancer regions (*14, 29*). We then analyzed the distances of sex-specific Brd4 binding sites to the nearest sex-specific H3K27ac-enriched enhancer regions and compared them to randomly selected Brd4 binding sites. As shown in **Figure 2C**, sex-specific Brd4 binding sites are significantly enriched at sex-specific H3K27ac enhancer regions ($p < 0.01$). Using sex-specific Brd4 binding sites that correlated with sex-specific H3K27ac-enriched enhancer regions within 1kb distance, we identified the closest upstream and downstream genes from the center of the Brd4 binding sites. This analysis revealed 351 male-specific genes and 384 female-specific genes. Pathway enrichment analysis on male-specific genes regulated by these sex-specific Brd4-marked enhancers revealed functional enrichment for glioma, neoplasm metastasis, metabolism, cell proliferation, chromosome aberrations and integrin signaling. Similar analysis on female-specific genes showed an enrichment in pathways involved in regulation of metabolic process, DNA repair-deficiency disorders, and semaphorin signaling **(Supplementary Table 1)**. Representative examples of two biologically relevant loci, Tet1 and

Sema3a, which correspond to male-specific and female-specific Brd4-marked enhancer regions respectively, are depicted in **Figure 2D and 2E** (*30*). Tet1 is the enzyme that converts 5-methyl-cytosine (5mC) into 5-hydroxymethylcytosine (5hmC). Tet1 is overexpressed in GBM, and the Tet1-catalyzed production of 5hmC is required for GBM tumorigenesis (*31*). Of note, Tet1 is regulated by the microRNA mir-21, another gene that is known to play a prominent role in GBM progression and that has a nearby male-specific super-enhancer **(Supplementary Figure 3A)**. Semaphorin 3a (Sema3a), originally identified as an axonal growth cone guidance molecule, has been described to have both pro-and anti-tumorigenic functions. For instance, Sema3a was shown to inhibit cell migration and initiate anti-angiogenic signaling cascades in breast cancer (*32*). In contrast, Sema3a was revealed to promote cell proliferation and vascular permeability in glioblastoma cells (*33, 34*). Additional examples of male-specific (Mir-21, and Rnh1) and female-specific (Rasgrp3 and Pax2) loci are illustrated in **Supplementary Figure 3A and 3B** respectively. This is the first demonstration of differential Brd4-bound enhancer usage by male and female cells of any kind and is consistent with earlier observations that these enhancers are key regulators of cell identity and fate (*13-15, 18, 35*).

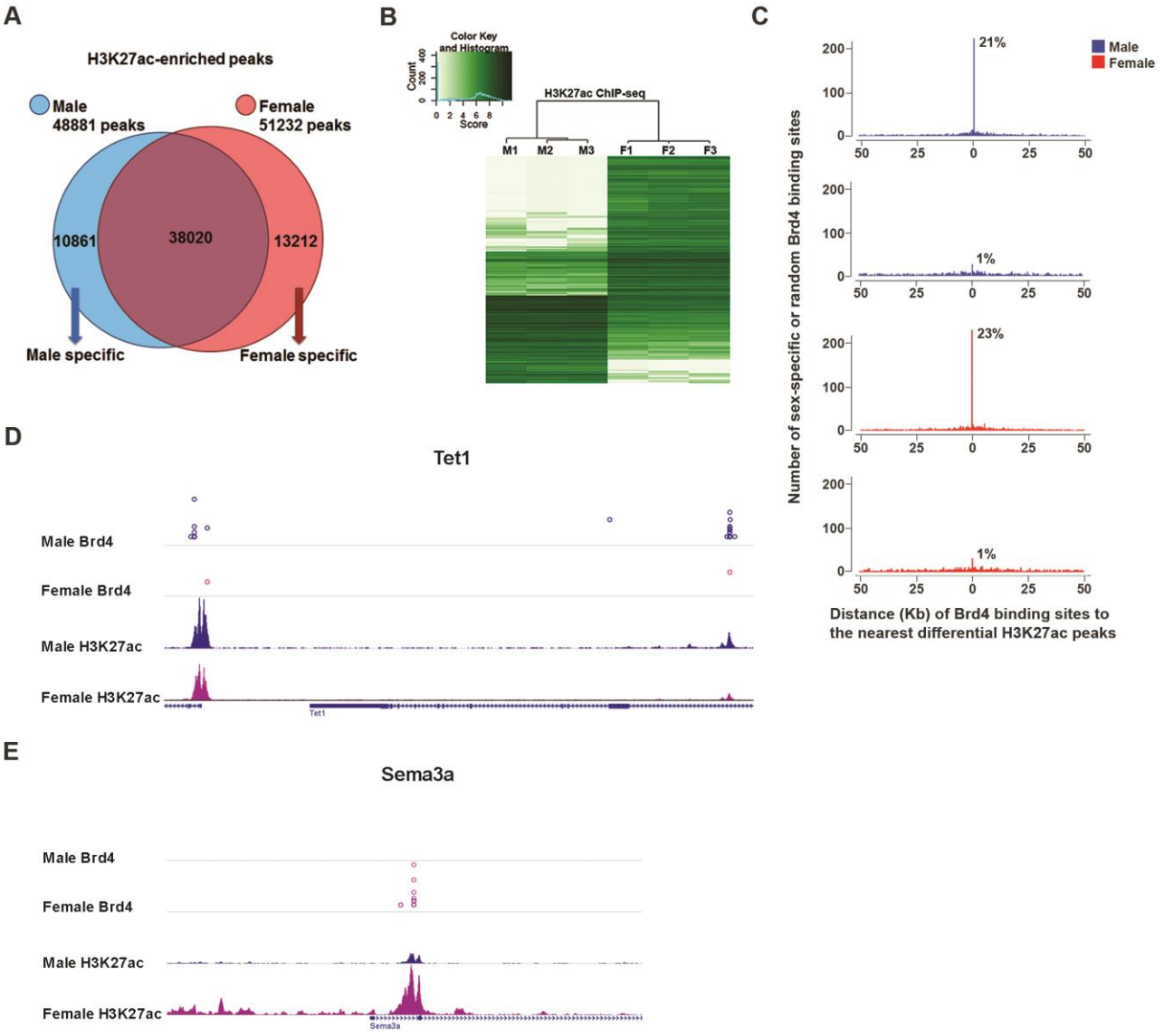

Figure 2. H3K27ac ChIP-seq analyses and Brd4 Transposon calling cards identify sexually dimorphic Brd4-bound enhancers in male and female GBM cells. (A) Venn diagram depicting the number of H3K27ac-defined enhancers in male and female cells; 10861 male-specific and 13212 female-specific H3K27ac-enriched peaks were identified. **(B)** Binding affinity heat map (read count) of differential H3K27ac-enriched regions in male and female GBM cells. Samples are clustered first by sex, then by replicate. Clusters of H3K27ac-enriched regions show distinct male and female patterns of H3K27ac binding levels. **(C)** Histograms of the distances of sex-specific Brd4 binding sites or randomly selected Brd4 binding sites to the nearest sex-specific H3K27ac enhancer region in male and female GBM cells receptively. Sex specific Brd4 binding-sites identified by transposon Calling Cards are significantly enriched around sex-specific H3K27ac enhancer regions compared to randomly selected Brd4 binding sites; 21% vs. 1% in male cells and 23% vs. 1% in female cells ($p < 0.01$). **(D, E)** Graphical representation of male and female-specific genes associated with differential Brd4 binding affinity and H3K27ac enrichment using epigenome browser. Shown are the tracks for Tet1 **(D)** and Sema3a **(E)** loci in GBM cells. The x-axis (blue arrows) of all tracks corresponds to genomic location of the gene. The y-axis of Calling Card tracks represents the log10 scale of sequencing reads for each insertion as indicated by circles (Tet1: min=0, max=3; Sema3a: min=0, max=3). The y-axis of ChIP-seq tracks represents the number of uniquely mapped reads. As the number of uniquely mapped reads collected from male and female samples were 26726687 and 26034293 respectively, the number was multiplied by 1.02 for female samples for comparison. (For male samples, Tet1: min=1, max=365; Sema3a: min=1, max=160).

Brd4-bound enhancers regulate sex differences in GBM

To further validate the transcriptional activation of sex-specific regulatory genes and networks by Brd4-bound enhancers, we treated our male and female GBM cells with the Brd4 antagonist JQ1. JQ1 is a thieno-triazolo-1,4-diazepine that displaces Brd4 from chromatin by competitively binding to the acetyl-lysine recognition pocket (*11, 23*). Treatment of acute myeloid leukemia cells with JQ1 caused a rapid release of Mediator 1 (Med1) from a subset of enhancer regions that were co-occupied by Brd4, leading to a decrease in the expression of neighboring genes (*36*). To investigate the functional activity of Brd4 at sexually dimorphic enhancer sites regulating expression of cancer-relevant genes, we treated male and female GBM cells with either vehicle (0.05% DMSO) or 500 nM JQ1 for 24 hours, then isolated genomic material for RNA-seq. Gene expression analysis on JQ1 treated cells revealed that Brd4 proximal genes are significantly downregulated compared to genes that are distal to Brd4 binding sites (p <0.01) indicating that JQ1 has a specific and directed effect on genes whose expression is driven by Brd4-bound enhancers **(Supplementary Figure 4).**

We next integrated our Brd4 Calling Cards, H3K27ac ChIP-seq and RNA-seq data to identify a set of sex-specific, Brd4 enhancer regulated genes. Candidate genes were identified by proximity to both a sex-specific Brd4 binding site and a sexually dimorphic H3K27ac enhancer region, and sensitivity to JQ1 (downregulation). These analyses identified 76 male-specific genes and 95 female-specific genes, which we refer to as sex-specific JQ1-sensitive genes. Similar to our previous pathway analyses, male-specific JQ1-sensitive genes demonstrated functional enrichment for neoplasm metastasis, tumor angiogenesis, integrin signaling pathway, and metabolic process, in addition to DNA-repair-deficiency disorders. Female-specific JQ1-sensitive

genes showed an enrichment in pathways involved in semaphorin signaling, chromosome aberrations, glioblastoma, regulation of transcription, and glucose metabolism disorders **(Table 1)**. These results are indicative of sex-specific transcriptional programs regulated by Brd4-bound enhancers. Identifying which specific pathways are critical to sex differences in GBM will require further functional studies.

Table 1. Differentially regulated genes and enriched pathways in male and female GBM cells identified by Brd4 Calling Cards, H3K27Ac ChIP_seq and downregulation following JQ1 treatment*

Pathway description	Genes	Adjusted *p*-value	# of Genes
Male GBM Cells: 76 genes			
Regulation of metabolic process	Lclat1, Rreb1, M1ap, Ak2, Akap6, Igfbp3, Loxl3, Prss22, St3gal4, Neu2, Nsmce2, Rad51b, Plaur, Tet1, Prkcb, Mettl18, Cfap61, Ces1f, Cbx5, Gria1, Tmpo, Bmper, Ces1g, Hsp90b1, Nenf, Mgat3, Parpbp, Eno3, Lipg, Ak5, Mthfd1l, Dpp6, Itpkb, Ccl9, Camk1d, Tshz3, Echdc3, Il34, Pif1, Rabggta, Glrp1, Pck2, Chst1	8.00E-03	43
Neoplasm metastasis	Rreb1, Slco2a1, Ak2, Akap6, Igfbp3, Loxl3, Kif26b, Col18a1, St3gal4, Neu2, Nsmce2, Rad51b, Plaur, Tet1, Prex2, Prkcb, Cbx5, Gria1, Kcnn4, Tmpo, Fam107a, Traf3ip2, Bmper, Ces1g, Hsp90b1, Rnh1, Lamc2, Mgat3, Dnm3, Parpbp, Gipc2, Eno3, Spp1, Lipg, Ak5, Dpp6, Fam84b, Ccl9, Sema5a, Il34, Pif1, Pck2, Fbn2	2.00E-03	43
DNA repair-deficiency disorders	Rreb1, Slco2a1, Ak2, Akap6, Igfbp3, Loxl3, Kif26b, Col18a1, St3gal4, Nsmce2, Slc35b3, Rad51b, Plaur, Tet1, Prkcb, Cbx5, Kcnn4, Tmpo, Ces1g, Hsp90b1, Lamc2, Mgat3, Parpbp, Gipc2, Spp1, Dpp6, Fam84b, Ccl9, Pif1, Fbn2, Chst1	1.00E-03	31
Tumor angiogenesis	Slco2a1, Kif26b, Col18a1, Plaur, Prkcb, Bmper, Spp1, Sema5a	1.00E-02	8
Integrin signaling	Col18a1, Plaur, Lamc2, Mgat3, Spp1, Ak5	2.00E-03	6
Female GBM Cells: 95 genes			
Chromosome aberrations	Sema3a, Trib2, Fer, Sema3e, Slc25a13, Mylk, Mrpl19, Grb10, Nrp2, Nfia, Rasgrp3, Acvr1, Dlx1, Mcm4, Pax2, Dut, Dync1i1, Col6a3, Itga4, Syt1, Mamdc2, Fbn1, Cd200, Dock1, Wnt2, Tslp, Npas3, Foxp1, Slc9a9, Kank1, Nrg1, St7, Wfdc1, Gja5, Mbnl1, Plcb4, Mkx, Gabrg3, Fmn1, Ikzf2	3.00E-03	40
Glioma / Glioblastoma	Sema3a, Sema3e, Tmem45a, Grb10, Nrp2, Kcna4, Nfia, Rasgrp3, Acvr1, Dlx1, Mcm4, S1pr1, Pax2, Dut, Rims2, Ptprb, Col6a3, Itga4, Syt1, Fbn1, Dock1, Dctd, Wnt2, Npas3, Tmeff1, Foxp1, Slc9a9, Ly75, Kif18a, Kank1, Nrg1, St7, Tacr1, Gja5, Plcb4, Ikzf2	0.00+-00	36 / 22
Glucose metabolism disorders	Sema3a, Fer, Sema3e, Slc25a13, Casq1, Txlnb, Grb10, Nrp2, Acvr1, Mcm4, S1pr1, Pax2, Col6a3, Itga4, Syt1, Fbn1, Cd200, Wnt2, Tslp, Npas3, Foxp1, Ly75, Slco1a5, Ankrd55, Nrg1, Tacr1, Gja5, Mbnl1, Plcb4, Ikzf2	7.00E-03	30
Regulation of transcription	Nfia, Acvr1, Dlx1, S1pr1, Pax2, Ptgs2os, Fbn1, Wnt2, Npas3, Foxp1, Nrg1, Lmcd1, Mkx, Ikzf2	7.00E-03	14
Semaphorin signaling	Sema3a, Fer, Sema3e, Nrp2	3.00E-03	4

* Subset of differentially regulated genes and enriched pathways in male and female GBM cells

In order to investigate the functional significance of sex-specific Brd4-bound enhancer usage and its effect on the tumorigenic phenotype, we again treated male and female GBM cells with the Brd4 antagonist JQ1 and then performed a panel of assays, including cell proliferation (growth assay), extreme limiting dilution assay to measure clonogenic cell (stem-like cell) frequency, and *in vivo* tumorigenesis. Following JQ1 treatment, male cells exhibited decreased proliferation and a growth phenotype equivalent to control female cells **(Figure 3A)**. In addition, treatment with JQ1 reproducibly abrogated the basal differences in clonogenic frequency between male and female GBM cells resulting in a decreased functional clonogenic cell fraction in male cells and an increased functional clonogenic cell fraction in female cells **(Figure 3B)**. This opposing sex-specific response to the inhibition of Brd4 is consistent with published data in breast and prostate cancer, wherein ectopic expression of Brd4 in breast cancer cells decreased invasiveness and tumor growth, while Brd4 inhibition decreased viability of prostate cancer cells (*25*, *37*, *38*). To confirm that these effects were mediated by Brd4-bound enhancers, we performed similar experiments using RVX-208, a BET inhibitor with selectivity for Brd2 and Brd3 (*39*). Treatment with 5μM RVX208 for 24 hours did not induce any significant change in the proliferation or clonogenic frequency of male and female cells **(Figure 3C and 3D)**.

To address the sex-specific effects of JQ1 treatment on *in vivo* tumorigenesis, we performed *in vivo* limiting dilution flank implantation studies. Each mouse received 5000, 100,000, 500,000 and 1 million DMSO or JQ1 treated male cells injected in 4 flank locations, and tumor growth was monitored blindly for 7-8 weeks with thrice weekly micrometer measurements in 3 dimensions **(Figure 3E)**. Flank implantation of JQ1-treated transformed male cells produced smaller tumors than control DMSO male implants **(Figure 3F)**. This effect was seen following only one dose of JQ1 prior to implantation, indicating that this robust response is maintained and

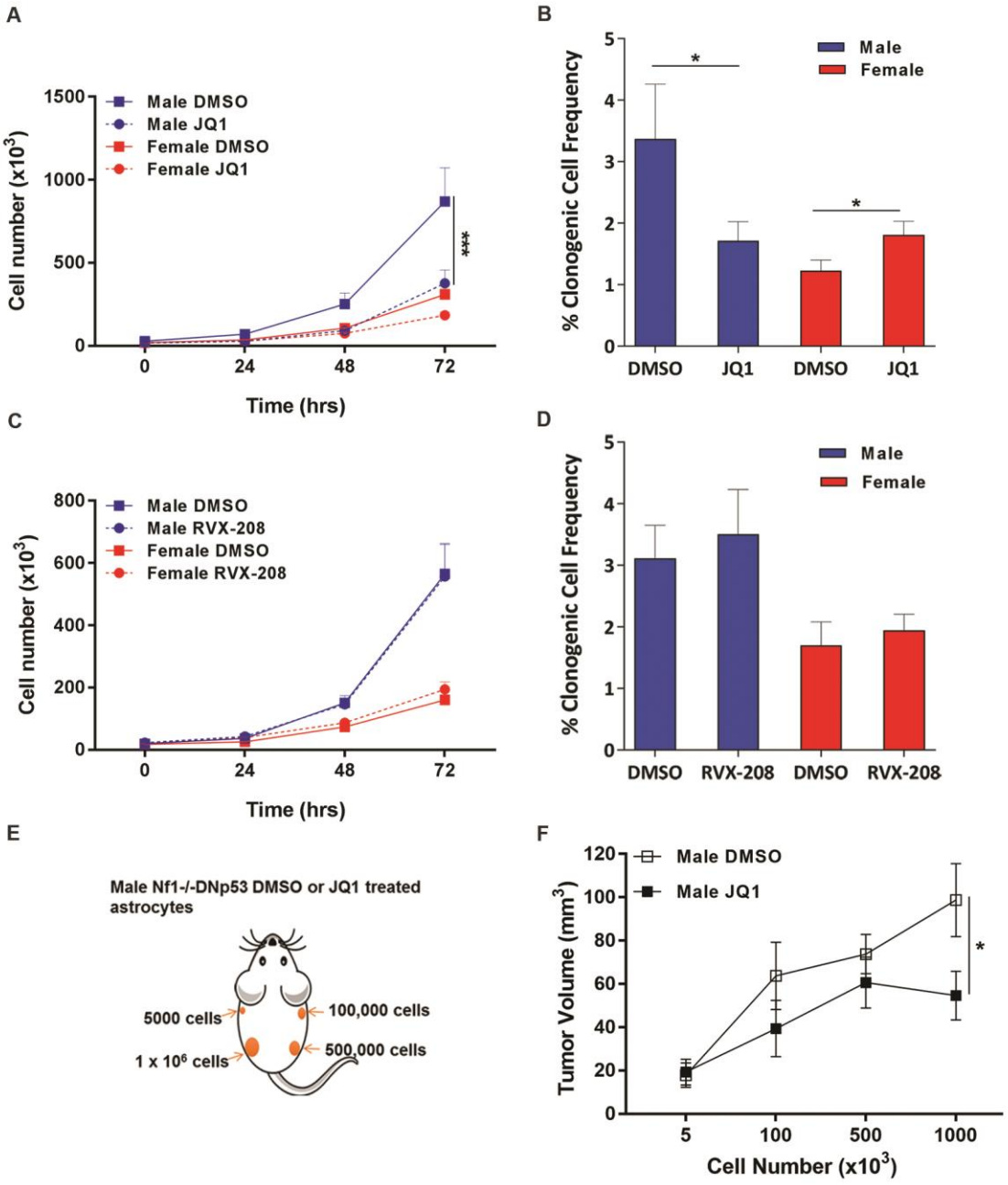

Figure 3. Brd4, not Brd2 or Brd3, bound enhancers drive sex differences in tumorigenic phenotype. (A, B) Tumorigenic phenotype, including proliferation **(A)** and clonogenic cell frequency (ELDA assay) **(B)**, were performed in GBM cells treated with DMSO (control) or JQ1 (500 nM for 24 hours). Male cells exhibited greater proliferation and clonogenic cell activity than female cells under control conditions. Following JQ1 treatment male cells exhibited a slower growth rate (A) and decreased stem-like cell frequency (B). Although no change was detected in their proliferation, female cells exhibited a significant increase in their stem-like cell frequency (B). **(C, D)** Tumorigenic phenotype, including proliferation **(C)** and clonogenic cell frequency (ELDA assay) **(D)**, were performed in GBM cells treated with DMSO (control) or RVX-208, a Brd2/3 selective antagonist (5μM for 24 hours). RVX-208 treatment did not induce any change in proliferation (C) or clonogenic activity (D) of male and female GBM cells. **(E)** Schematic representation of flank implantation of 4 different amounts of DMSO or JQ1 (500 nM for 24 hours) treated transformed male GBM cells. **(F)** Male tumors were significantly inhibited in their *in vivo* growth following JQ1 treatment compared to DMSO treatment. (*=p <0.05 ***=p <0.01 as determined by two-tailed t-test).

manifested at the epigenetic level. Taken together, these remarkable results demonstrate for the first time that the sex differences in the tumorigenic phenotype we observe in GBM cells are mediated by differential Brd4-marked enhancers, and that the response to JQ1 is sex-dependent.

Genetic knockdown of Brd4 recapitulates the effects of JQ1 treatment on tumorigenic phenotype

The primary target of JQ1 is thought to be Brd4, but it also has some activity against Brd2, although with much higher IC50. Therefore, we sought to determine whether the efficacy of JQ1 was due to inhibition of Brd4 or inhibition of Brd2. We used shRNAs specific to either Brd4 or Brd2 then evaluated the effect on the tumorigenic phenotype of male and female GBM cells. As shown in **Figure 4A**, mRNA expression levels of both Brd4 and Brd2 were partially silenced in male and female GBM cells after infection with lentiviral shRNAs. Of note, Brd4 mRNA4 levels were equivalent between male and female GBM cells under basal conditions. The growth assay demonstrated that knockdown of Brd4 with shRNAs recapitulates the effects of JQ1 and decreases proliferation in male but not female cells **(Figure 4B)**. While JQ1 treatment completely abrogated the basal differences in growth between male and female, this is not the case here, likely due to the fact that genetic knockdown was only partial. Knockdown of Brd2 with shRNAs did not affect growth in either male or female cells, which is consistent with our earlier RVX-208 results **(Figure 4C)**. Moreover, male GBM cells with knockdown of Brd4 exhibited a decrease in clonogenic frequency whereas female cells displayed an increase in clonogenic frequency. No change in clonogenic frequency was observed following Brd2 knockdown **(Figure 4D)**. Altogether, these data further affirm the role of Brd4 as a mediator of sex differences in GBM tumorigenic phenotype.

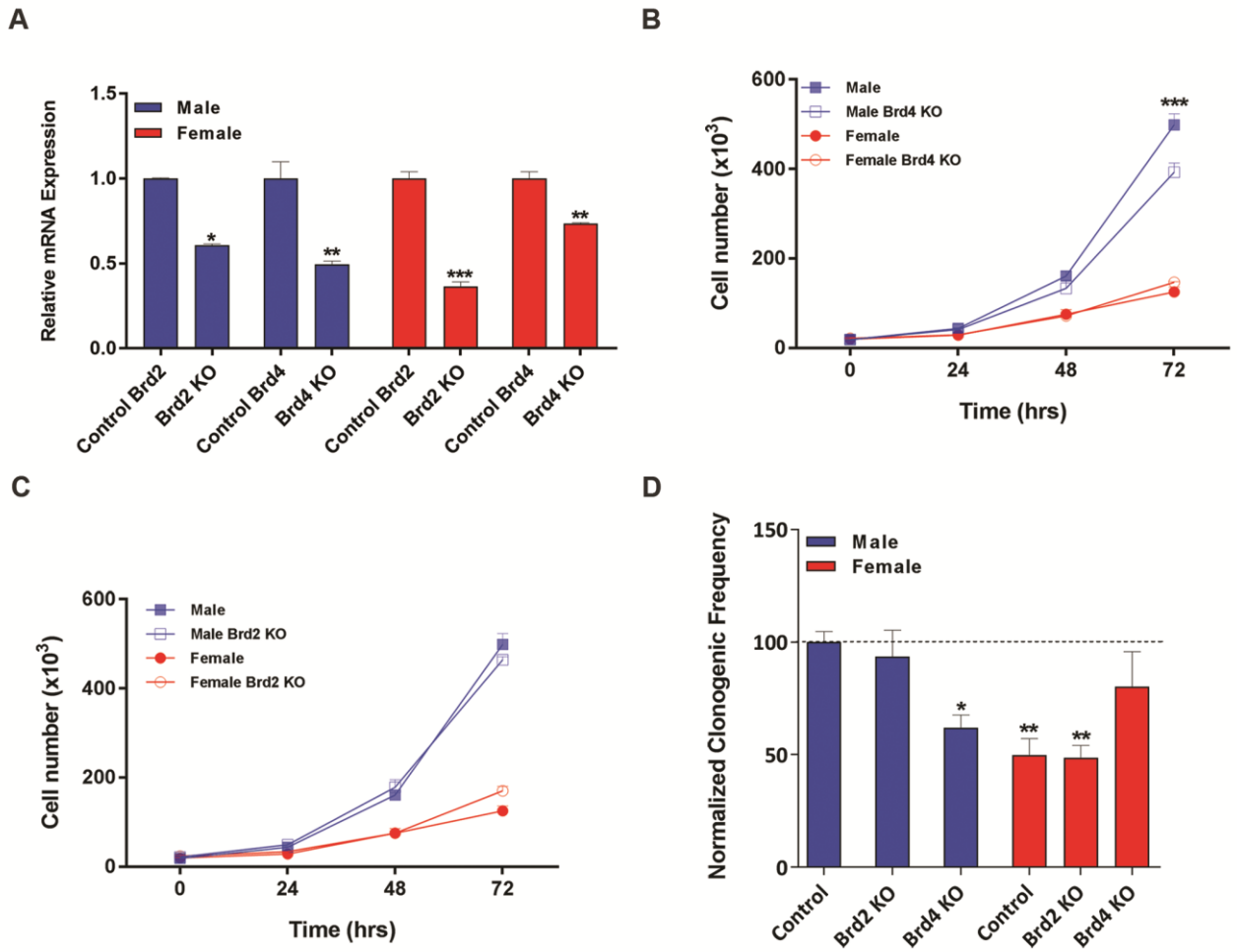

Figure 4. Inhibition of Brd4 with shRNAs suppresses growth and clonogenic frequency in male GBM cells while Brd2 inhibition exhibits no effect. (A) Real-time quantitative PCR of Brd2 and Brd4 mRNA expression confirms knockdown using specific lentiviral shRNAs infection. **(B-D)** Sub-threshold tumorigenic phenotypes, including proliferation **(B, C)** and clonogenic cell frequency **(D)**, were performed in shRNA knockdown and control GBM cells. Following Brd4 shRNAs infection, male cells showed a decrease in growth (B) and clonogenic frequency (D), while female cells showed an increase in clonogenic frequency (D) similar to the JQ1 sex-specific effect. In contrast, inhibition of Brd2 did not produce any change in proliferation (C) or clonogenic frequency (D) in male and female GBM cells. All treatment groups were normalized to male control clonogenic frequency levels (*=p <0.05 **=p <0.01 as determined by one-way ANOVA).

Brd4 expression levels in TCGA human GBM samples correlate with sex-specific survival outcomes

To investigate the effect of Brd4 expression on sex-specific survival outcomes in human GBM, we obtained gene expression data from 151 (98 males and 53 females) TCGA glioblastoma samples, converted the expression value of Brd4 into a z-score specific to the sex of the patient (**Supplementary Figure 5**) and stratified the patients into a high-expression group (z-score > 1.0) and low-expression group (z-score < -1.0). We analyzed the effects of Brd4 expression on patient overall survival (OS) using the Kaplan-Meier method (*40*). While high Brd4 expression group had no effect on survival (**Supplementary Figure 6A & B**), low Brd4 expression was associated with shortened survival in females (OS median - 5.39 months) compared to males (OS median - 16.59 months, $p = 0.07$) (**Figure 5**). This is consistent with our findings in our mouse GBM model, in which treatment with the Brd4 inhibitor JQ1 abrogated the tumorigenic phenotype in male cells, but enhanced it in female cells. Additionally, this data is consistent with previously published breast, endometrial and prostate cancer studies revealing that in women with estrogen receptor positive breast cancer (*37*) or endometrial cancer (*38*) low Brd4 expression is correlated with worsened survival. This is in contrast to men with prostate cancer in whom low levels of Brd4 are associated with improved survival (*25, 38*). Altogether, the consistency between our mouse data, the GBM TCGA data, and published breast and prostate cancer studies, provides strong evidence for the context-dependent, sex-specific dual role of Brd4 in regulating gene expression programs in oncogenesis.

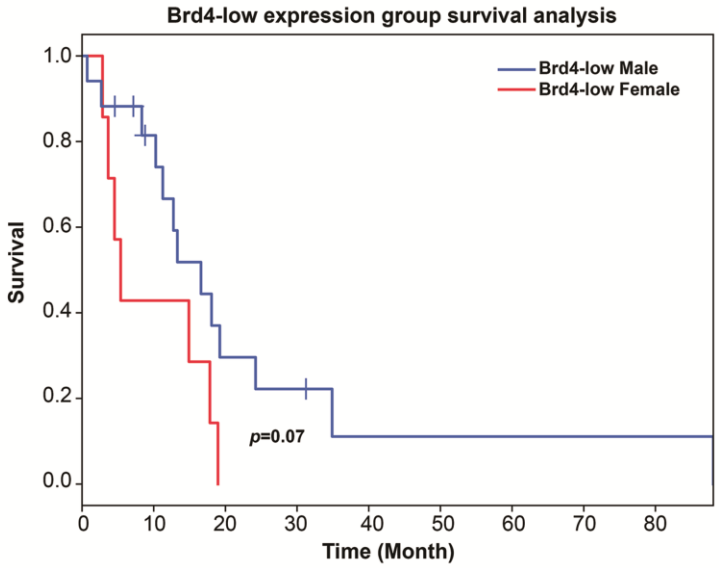

Figure 5. Sex-specific survival differences in Brd4 low-expression group from TCGA GBM data sets. Female GBM patients with low Brd4 expression (z-score < -1.0) have decreased survival, (median OS - 5.39 months), compared to male GBM patients with low Brd4 expression (z-score < -1.0, median OS - 16.59 months; p=0.07).

In conclusion, these data demonstrate for the first time that cell intrinsic sex identity is mediated by sex differences in Brd4-marked enhancer usage. In the model utilized here, the differential usage of Brd4-bound enhancers mediated important sex differences in a GBM tumorigenic phenotype. Additionally, the response to JQ1 treatment was shown to be sex-dependent. Since bromodomain inhibitors are currently being evaluated in a number of clinical trials, understanding this phenomenon is of critical importance, both for the interpretation of existing trials and to guide better application of these drugs. Increasing our knowledge of these sex-specific genetic and epigenetic mechanisms will lead to a greater understanding of cancer biology and its relationship to normal development, as well as identify novel therapeutic targets to improve outcome for all patients with GBM and potentially other cancers that exhibit substantial sex differences in incidence or outcome.

References and notes

1. C. Ober, D. A. Loisel, Y. Gilad, Sex-specific genetic architecture of human disease. *Nat Rev Genet* **9**, 911-922 (2008).

2. Q. T. Ostrom *et al.*, The epidemiology of glioma in adults: a "state of the science" review. *Neuro Oncol* **16**, 896-913 (2014).

3. C. Ang, M. C. Guiot, A. V. Ramanakumar, D. Roberge, P. Kavan, Clinical significance of molecular biomarkers in glioblastoma. *Can J Neurol Sci* **37**, 625-630 (2010).

4. Q. T. Ostrom *et al.*, CBTRUS Statistical Report: Primary Brain and Other Central Nervous System Tumors Diagnosed in the United States in 2009-2013. *Neuro Oncol* **18**, v1-v75 (2016).

5. R. Siegel *et al.*, Cancer treatment and survivorship statistics, 2012. *CA Cancer J Clin* **62**, 220-241 (2012).

6. R. Siegel, D. Naishadham, A. Jemal, Cancer statistics for Hispanics/Latinos, 2012. *CA Cancer J Clin* **62**, 283-298 (2012).

7. T. Sun, N. M. Warrington, J. B. Rubin, Why does Jack, and not Jill, break his crown? Sex disparity in brain tumors. *Biol Sex Differ* **3**, 3 (2012).

8. M. T. Dorak, E. Karpuzoglu, Gender differences in cancer susceptibility: an inadequately addressed issue. *Front Genet* **3**, 268 (2012).

9. T. Sun *et al.*, Sexually dimorphic RB inactivation underlies mesenchymal glioblastoma prevalence in males. *J Clin Invest* **124**, 4123-4133 (2014).

10. M. M. McCarthy, B. M. Nugent, At the frontier of epigenetics of brain sex differences. *Front Behav Neurosci* **9**, 221 (2015).

11. P. Filippakopoulos *et al.*, Selective inhibition of BET bromodomains. *Nature* **468**, 1067-1073 (2010).

12. Y. Zhang *et al.*, Model-based analysis of ChIP-Seq (MACS). *Genome Biol* **9**, R137 (2008).

13. J. M. Dowen *et al.*, Control of cell identity genes occurs in insulated neighborhoods in mammalian chromosomes. *Cell* **159**, 374-387 (2014).

14. D. Hnisz *et al.*, Super-enhancers in the control of cell identity and disease. *Cell* **155**, 934-947 (2013).

15. D. Hnisz *et al.*, Convergence of developmental and oncogenic signaling pathways at transcriptional super-enhancers. *Mol Cell* **58**, 362-370 (2015).

16. S. Ounzain, T. Pedrazzini, Super-enhancer lncs to cardiovascular development and disease. *Biochim Biophys Acta* **1863**, 1953-1960 (2016).

17. S. C. Parker *et al.*, Chromatin stretch enhancer states drive cell-specific gene regulation and harbor human disease risk variants. *Proceedings of the National Academy of Sciences of the United States of America* **110**, 17921-17926 (2013).

18. W. A. Whyte *et al.*, Master transcription factors and mediator establish super-enhancers at key cell identity genes. *Cell* **153**, 307-319 (2013).

19. P. Filippakopoulos, S. Knapp, Targeting bromodomains: epigenetic readers of lysine acetylation. *Nature reviews. Drug discovery* **13**, 337-356 (2014).

20. J. Alsarraj *et al.*, Deletion of the proline-rich region of the murine metastasis susceptibility gene Brd4 promotes epithelial-to-mesenchymal transition- and stem cell-like conversion. *Cancer research* **71**, 3121-3131 (2011).

21. T. Wu, M. E. Donohoe, The converging roles of BRD4 and gene transcription in pluripotency and oncogenesis. *RNA & disease* **2**, (2015).

22. T. Wu, H. B. Pinto, Y. F. Kamikawa, M. E. Donohoe, The BET family member BRD4 interacts with OCT4 and regulates pluripotency gene expression. *Stem cell reports* **4**, 390-403 (2015).

23. J. E. Delmore *et al.*, BET bromodomain inhibition as a therapeutic strategy to target c-Myc. *Cell* **146**, 904-917 (2011).

24. J. Loven *et al.*, Selective inhibition of tumor oncogenes by disruption of super-enhancers. *Cell* **153**, 320-334 (2013).

25. A. Urbanucci *et al.*, Androgen Receptor Deregulation Drives Bromodomain-Mediated Chromatin Alterations in Prostate Cancer. *Cell reports* **19**, 2045-2059 (2017).

26. I. Ali, G. Choi, K. Lee, BET Inhibitors as Anticancer Agents: A Patent Review. *Recent Pat Anticancer Drug Discov*, (2017).

27. H. Wang, D. Mayhew, X. Chen, M. Johnston, R. D. Mitra, Calling Cards enable multiplexed identification of the genomic targets of DNA-binding proteins. *Genome Res* **21**, 748-755 (2011).

28. H. Wang, D. Mayhew, X. Chen, M. Johnston, R. D. Mitra, "Calling cards" for DNA-binding proteins in mammalian cells. *Genetics* **190**, 941-949 (2012).

29. R. Di Micco *et al.*, Control of embryonic stem cell identity by BRD4-dependent transcriptional elongation of super-enhancer-associated pluripotency genes. *Cell reports* **9**, 234-247 (2014).

30. X. Zhou *et al.*, The Human Epigenome Browser at Washington University. *Nat Methods* **8**, 989-990 (2011).

31. H. Takai *et al.*, 5-Hydroxymethylcytosine plays a critical role in glioblastomagenesis by recruiting the CHTOP-methylosome complex. *Cell reports* **9**, 48-60 (2014).

32. D. R. Bielenberg *et al.*, Semaphorin 3F, a chemorepulsant for endothelial cells, induces a poorly vascularized, encapsulated, nonmetastatic tumor phenotype. *J Clin Invest* **114**, 1260-1271 (2004).

33. T. Bagci, J. K. Wu, R. Pfannl, L. L. Ilag, D. G. Jay, Autocrine semaphorin 3A signaling promotes glioblastoma dispersal. *Oncogene* **28**, 3537-3550 (2009).

34. L. Treps *et al.*, Extracellular vesicle-transported Semaphorin3A promotes vascular permeability in glioblastoma. *Oncogene* **35**, 2615-2623 (2016).

35. Z. Najafova *et al.*, BRD4 localization to lineage-specific enhancers is associated with a distinct transcription factor repertoire. *Nucleic acids research* **45**, 127-141 (2017).

36. A. S. Bhagwat *et al.*, BET Bromodomain Inhibition Releases the Mediator Complex from Select cis-Regulatory Elements. *Cell reports* **15**, 519-530 (2016).

37. N. P. Crawford *et al.*, Bromodomain 4 activation predicts breast cancer survival. *Proceedings of the National Academy of Sciences of the United States of America* **105**, 6380-6385 (2008).

38. H. Janouskova *et al.*, Opposing effects of cancer-type-specific SPOP mutants on BET protein degradation and sensitivity to BET inhibitors. *Nat Med* **23**, 1046-1054 (2017).

39. S. Picaud *et al.*, RVX-208, an inhibitor of BET transcriptional regulators with selectivity for the second bromodomain. *Proceedings of the National Academy of Sciences of the United States of America* **110**, 19754-19759 (2013).

40. J. E. Ippolito, A. K. Yim, J. Luo, P. Chinnaiyan, J. B. Rubin, Sexual dimorphism in glioma glycolysis underlies sex differences in survival. *JCI Insight* **2**, (2017).

41. T. E. Reddy *et al.*, Genomic determination of the glucocorticoid response reveals unexpected mechanisms of gene regulation. *Genome Res* **19**, 2163-2171 (2009).

42. A. Dobin *et al.*, STAR: ultrafast universal RNA-seq aligner. *Bioinformatics* **29**, 15-21 (2013).

43. S. Anders, P. T. Pyl, W. Huber, HTSeq--a Python framework to work with high-throughput sequencing data. *Bioinformatics* **31**, 166-169 (2015).

44. M. I. Love, W. Huber, S. Anders, Moderated estimation of fold change and dispersion for RNA-seq data with DESeq2. *Genome Biol* **15**, 550 (2014).

45. B. Langmead, S. L. Salzberg, Fast gapped-read alignment with Bowtie 2. *Nat Methods* **9**, 357-359 (2012).

46. C. S. Ross-Innes *et al.*, Differential oestrogen receptor binding is associated with clinical outcome in breast cancer. *Nature* **481**, 389-393 (2012).

47. R. a. B. Stark, G., DiffBind: differential binding analysis of ChIP-Seq peak data. (2011).

Acknowledgments: This work was supported by NIH RO1 CA174737 (JBR), Joshua's Great Things (JBR), and The Children's Discovery Institute (RM). We thank the Genome Technology Access Center in the Department of Genetics at Washington University School of Medicine for help with genomic analysis. The Center is partially supported by NCI Cancer Center Support Grant #P30 CA91842 to the Siteman Cancer Center and by ICTS/CTSA Grant# UL1 TR000448 from the National Center for Research Resources (NCRR), a component of the National Institutes of Health (NIH), and NIH Roadmap for Medical Research. This publication is solely the responsibility of the authors and does not necessarily represent the official view of NCRR or NIH.

Materials and methods

RNA-sequencing

Male and female GBM cells (Nf-/-;DNp53 astrocytes) were generated as previously reported (Sun et al., 2015) and grown in DMEM/F12 media supplemented with 10% FBS and 1% penicillin-streptomycin. Total RNA was isolated from male and female GBM cells that were treated with DMSO (0.05%) or JQ1 (500 nM for 24 hours) using the RNeasy Mini Kit from Qiagen, following the kit protocol (Hilden, Germany). PolyA Selection was performed to create RNA Seq libraries. Cell mRNA was extracted from total RNA using a Dynal mRNA Direct kit. The quantity of RNA was measured using a spectrophotometer (NanoDrop 2000c; Thermo Scientific). Samples with an RNA concentration A260/A280 ≥1.8 ng/µl, and purity A230/A260 ≥ 2.0 ng/µl were selected. The Agilent 2100 Bioanalyzer was used to determine the RNA integrity number. The degradation level was identified using the RNA 6000 Nano LabChip kit (Agilent). Samples with RNA integrity number > 9.8 were further processed using TruSeq mRNA Library Preparation Kit (Illumina) and then sequenced on a HiSeq 25000 (Illumina).

Chromatin immunoprecipitation sequencing (ChIP-seq) for H3K27ac

10 million male and female GBM cells were treated with 0.05% DMSO or 500 nM JQ1 for 24 hours. Following treatment, cells were then prepared for various downstream analysis including ChIP-seq for H3K27ac. Briefly, cells were fixed in 1% formaldehyde prepared in media and incubated for 10 minutes at room temperature with gentle rocking. Fixation was quenched by the addition of glycine to a final concentration of 125 mM and incubation for 10 minutes at room

temperature with gentle rocking. Cells were then washed with cold PBS and harvested by scraping in 5 ml of cold PBS. Cells were then transferred to 15 mL conical tubes and pelleted with a 5-minute spin (1,000g) at 4ºC. ChIP-seq libraries were constructed as previously described (*41*), with an antibody that recognizes H3K27Ac (Active Motif, 39133, rabbit polyclonal). Sonication was performed on an Epishear probe-in sonicator (Active Motif) at 40% amplitude for 8 cycles of 30 seconds with 30 seconds of rest between each cycle. ChIP-seq libraries were constructed with sample-specific barcodes, and pooled before sequencing on a HiSeq 2500 (Illumina).

Transposon calling cards sequencing for Brd4

Male and female GBM cells were grown to 50% confluence (200K cells/T25 flask). On the day of transfection and 30 minutes before applying complexes, media was replaced with DMEM without FBS and antibiotics. Transfection complexes containing 3 µg of PB helper DNA with a PB-Brd4 fusion and/or 3 µg of PB donor DNA with a puromycin selection marker and Lipofectamine LTX/Plus Reagent (Invitrogen) were applied to cells for 12-18 hours at a culturing condition of 37 °C and 5% CO_2. Cells were then allowed to recover in fresh medium containing DMEM/F12 with 10% FBS and 1% penicillin-streptomycin for another 24-48 hours. Cells were then expanded into T75 flasks and selected using puromycin at a concentration of 2.5 µg/ml for 3 days. DNA was extracted from puromycin resistant cells and processed by transposon calling card protocol as previously described (*28*). Briefly, DNA sample was divided into three 2-mg aliquots, each digested by MspI, Csp6I, or TaqI individually. Digested DNA was ligated overnight at 15°C in dilute solution to encourage self-ligation. After ethanol precipitation, self-ligated DNA was resuspended in 30 ml ddH2O and used as template in an inverse PCR. Primers that anneal to PB donor sequences were used to amplify the genomic regions flanking PB, and adapter sequences

that allow the PCR products to be sequenced on the Illumina genome analyzer were added. The PCR products were purified using the QIAquick PCR purification kit (Qiagen) and diluted into 10 nM concentration. For each sample, the same amount of PCR product from digestion with each restriction endonuclease was pooled and submitted for Illumina sequencing (HiSeq 2500).

Sequencing data alignment and analysis

RNA-seq data sets were aligned to the transcriptome and the whole-genome with STAR (*42*). Genes or exons were filtered for just those that were expressed. A gene count table for all the genes in each sample was generated using HTSeq (*43*). Differential gene expression between pairs of samples was computed using DESeq2 and was filtered by FDR < 0.05 for differentially expressed genes (*44*).

ChIP-seq data sets for H3K27ac were aligned to the murine genome build mm10 using Bowtie2 and only uniquely aligning reads were used (*45*). Regions of enrichment of H3K27ac over background were calculated using the MACS version (2.1.0) peak finding algorithm (*12*). An adjusted *p*-value threshold of enrichment of 0.01 was used for all data sets. The resulting peak files were used as inputs for DiffBind (version 3.5) to derive consensus peak sets (*46, 47*). The differential enrichment of H3K7Ac signals between male and female analysis was carried out with Diffbind using DESeq2 (method = DBA_DESEQ2) with libraries normalized to total library size.

Transposon calling cards data sets were aligned to the murine genome build mm10 using Bowtie2 (*45*). The Brd4 binding site was identified by using an established algorithm (*28*). Briefly, the Brd4-directed PB insertions were clustered using a hierarchical clustering algorithm to identify insertions within 2500 bp and then modeled as a Poisson distribution, with the number of

independent insertions in the "transposase-alone" experiment in the same genomic window setting the expectation. The *p*-value is then calculated from cumulative distribution function given the observed number of independent insertions in the Brd4-directed experiment.

To identify the sites with an excess of Brd4 insertions in male GBM cells relative to female cells, we used the algorithm from ChIP-Seq peaks caller MACS (*12*) but modified for the analysis of calling card data. First, the transposon insertions were grouped by hierarchical clustering. Then, peaks with an excess of insertions in the male sample were identified by computing lambda, the number of insertions per TTAA expected from the female sample by taking the maximum lambda calculated from the number of insertions in the female peak, or in a 1kb, 5kb or 10kb window centered at that peak.. We computed a *p*-value based on the expected number of insertions (lamda × number of TTAAs in peak × number of insertions in peak). To identify the sites with an excess of Brd4 insertions in female GBM cells relative to male cells, we performed the same analysis, substituting the male and female data sets.

Pathway analysis

Pathway enrichment analysis for differentially regulated genes was performed using a combination of KEGG pathway and Genomatix Pathway System (GePS). GePS uses information extracted from public and proprietary databases to display canonical pathways and or to create and extend networks based on literature data. These sources include NCI-Nature Pathway Interaction Database, Biocarta, Reactome, Cancer Cell Map, and the ENCODE Transcription Factor project data. All data for pathway analyses are presented with adjusted corrected *p*-values.

Growth assays

Growth kinetics of male and female GBM cells (Nf-/-;DNp53 astrocytes) treated with DMSO (0.05%), JQ1 (500 nM), or RVX-208 (5µM) for 24 hours or shRNAs were examined by counting live cell number using an automated T4 cell counter as previously described with minor modifications (Sun et al., 2015). Briefly, cells were harvested and plated in a 6-well plate at a density of 2 x 10^4 cells/well (2 technical replicates per treatment/genotype/time point). 4 hours post plating, cells were harvested by trypsinization and counted in the presence of trypan blue. This time point was designated as the starting point (T0) of the time course. Cells were then harvested and counted every 24 hours for a total of 4 days (24, 48, 72 and 96 hours). This experiment was repeated three times.

Clonogenic cell frequency assay: Extreme Limiting Dilution Assays (ELDA analysis)

Clonogenic capacity of male and female GBM cells (Nf-/-;DNp53 astrocytes) treated with DMSO (0.05%), JQ1 (500 nM), or RVX-208 (5µM) for 24 hours or shRNAs was assayed by the Extreme Limiting Dilution Assay (ELDA). The frequency of clonogenic stem cells was evaluated by the cells' ability to form tumor-sphere in low-adherent conditions as previously reported (Sun et al., 2015). Briefly, cells were harvested into a single cell suspension and plated in neurosphere media containing EGF and FGF on 96-well ultra-low attachment plates in a serial dilution ranging from 3000 cells/well to 1 cell/well (3000, 600, 120, 24, 5 and 1 cells; n=14/cell density). Sphere formation was measured 7 days after plating. Clonogenic stem-like cell frequency was analyzed using the Extreme Limiting Dilution Analysis (http://bioinf.wehi.edu.au/software/elda/).

In vivo tumorigenesis: flank implantation

Flank tumors were generated by implanting GBM astrocytes at various cell numbers subcutaneously into left and right side flanks (top and bottom). These cells were treated with EGF for one week (50ng/ml) followed with a 0.05% DMSO or 500 nM JQ1 treatment for 24 hours. 1 million, 500,000, 100,000 or 5000 cells were then harvested and resuspended in 100 µl of 1:1 media to matrigel (BD Biosciences) and injected into the four flanks of mice. Mice were monitored weekly and tumor growth was monitored blindly for 7-8 weeks with thrice weekly micrometer measurements in 3 dimensions. Animals were used in accordance with an animal studies protocol (no. 20150177) approved by the Animal Studies Committee of the Washington University School of Medicine per the recommendations of the Guide for the Care and Use of Laboratory Animals (NIH).

shRNAs lentiviral infection and knockdown of Brd2 and Brd4

Brd2 and Brd4 knockdown lines were generated by infecting male and female GBM cells (Nf-/-;DNp53 astrocytes) with lentiviral shRNAs against Brd2 or Brd4. We used a pool of 5 shRNAs for Brd4 as well as Brd2. Both Brd2 and Brd4 Knockdown lines were selected with puromycin (2.5 µg/ml) in media for 1-2 weeks and the survivors were expanded for downstream target knockout analysis.

Quantitative Real-Time PCR

Total RNA was isolated using Trizol RNA extraction method (Invitrogen, CA) from male and female GBM cells (Nf-/-;DNp53 astrocytes) infected with shRNAs lentivirus against Brd2 or

Brd4. cDNA was generated using the QuantiTect Reverse Transcription Kit (Qiagen). Quantitative RT-PCR was performed using gene-specific primers and iTaq SYBR Green PCR master mix (Biorad, CA). Data was analyzed by standard ΔCq method (2-ΔΔCq) where ΔCq is the difference between the gene of interest and GAPDH control Cq value.

Statistical analysis

All experiments in this study were carried out at least three times. ANOVA and two-tailed Student's t-test were used to compare the differences in all functional measurements between JQ1, RVX-208 and control group (DMSO), and a p-value < 0.05 was considered statistically significant.

To test if upregulated genes in male cells compared to female cells and vice versa are significantly enriched for H3K27ac binding, the normalized H3K27ac signal intensities (reads) from 1kb upstream of the gene start site to 1kb downstream of the end of the gene were used for the correlation analysis. A paired Mann-Whitney-Wilcoxon test was used to compare normalized H3K27ac signal intensities between male and females cells and a p-value less than 0.01 was considered statistically significant.

To investigate if Brd4-proximal genes are significantly downregulated upon JQ1 treatment compared to Brd4-distal genes, we first defined Brd4 proximal genes as the closest genes to Brd4 binding sites and Brd4 distal genes as genes located near sites that are not enriched for Brd4 binding sites (353 male genes and 292 female genes). The expression profiles before and after JQ1 treatment of Brd4 proximal and distal genes were used for a Mann-Whitney-Wilcoxon test for male and female respectively and a p-value less than 0.01 was considered statistically significant.

TCGA human GBM data analysis

Level 3 RNA-seq gene expression data for TCGA GBM samples were obtained from the Broad GDAC Firehose data portal. Clinicopathologic data for the GBM samples were obtained from the cBioPortal for cancer genomics. Only tumor samples that represented primary tumors were used and recurrent tumor samples were excluded from the analysis. In total, gene expression and clinicopathologic data of 98 males and 53 females were used in this analysis.

To identify sex differences in overall survival (OS) outcomes for Brd4 in GBM patients, male and female patients were stratified into different expression groups and differences in survival outcomes among groups were then assessed (*40*). The Brd4 gene expression value was first transformed into a z-score that was specific to the sex of the patient, and the patients were grouped into high expression group ($Z > 1.0$) and low expression group ($Z < -1.0$). The patient groups of each sex were associated with survival endpoints by the Kaplan-Meier method, and log-rank test was used to compare survival difference among groups. High expression and low expression groups were analyzed separately.